www.czasopisma.pan.pl PAN POLSKA AKADEMIA NAUK www.journals.pan.pl

Arch. Metall. Mater. **66** (2021), 1, 223-228

DOI: 10.24425/amm.2021.134779

I. SCHINDLER[1*], P. OPĚLA[1], P. KAWULOK[1], M. SAUER[1], S. RUSZ[1],
D. KUC[2], K. RODAK[2]

HOT DEFORMATION ACTIVATION ENERGY OF METALLIC MATERIALS INFLUENCED BY STRAIN VALUE

Suitable and complete sets of stress-strain curves significantly affected by dynamic recrystallization were analyzed for 11 different iron, copper, magnesium, titanium or nickel based alloys. Using the same methodology, apparent hot deformation activation energy Q_p and Q_{ss} values were calculated for each alloy based on peak stress and steady-state stress values. Linear dependence between quantities Q_p and Q_{ss} was found, while Q_p values are on average only about 6% higher. This should not be essential in predicting true stress of a specific material depending on the temperature-compensated strain rate and strain.

Keywords: Flow stress curves, Steady state, Metallic materials, Hot deformation activation energy

1. Introduction

The apparent activation energy value Q ($J \cdot mol^{-1}$) in hot forming is considered as an important material constant, used primarily for the calculation of the Zener-Hollomon parameter Z (s^{-1}) representing the temperature-compensated strain rate [1]. Its knowledge for the given material enables, among others, to predict effectively the maximum flow stress value or the strain value corresponding to the start of the dynamic recrystallization at the given temperature T (K) and strain rate $\dot{e}$ (s^{-1}) – see e.g. [2,3]. The Q-value is ideally the material constant depending only on the chemical composition and microstructure of the particular material. The hyperbolic law in Arrhenius type equation is conventionally used for its determination [4]:

$$\dot{e} = C \cdot \exp\left(\frac{-Q}{R \cdot T}\right) \cdot \left[\sinh\left(\alpha \cdot \sigma_p\right)\right]^n \tag{1}$$

where C (s^{-1}), n (-) and α (MPa^{-1}) are other material constants, $R = 8.314$ $J \cdot mol^{-1} \cdot K^{-1}$ and σ_p (MPa) is flow stress corresponding to the peak stress on the individual stress-strain curve. This relationship is often solved by a simple graphic method, based on the repeatedly used linear regression. A particularity of the hyperbolic function is used in this calculation that simplifies the Eq. (1) for low stress values (i.e. $\alpha \cdot \sigma_p < 0.8$) into the form of the Arrhenius power law [5]:

$$\dot{e} = C_1 \cdot \exp\left(\frac{-Q}{R \cdot T}\right) \cdot {\sigma_p}^n \tag{2}$$

and, vice versa, for high stress values (i.e. $\alpha \cdot \sigma_p > 1.2$) into the form of the exponential law [5]:

$$\dot{e} = C_2 \cdot \exp\left(\frac{-Q}{R \cdot T}\right) \cdot \exp\left(\beta \cdot \sigma_p\right) \tag{3}$$

where C_1, C_2 and β are the material constants. The constant a in Eq. (1) is given by the relationship $\alpha = \beta/n$. For a chosen high-temperature level (i.e. for low stress values) the constant n is determined by the linear regression of the experimentally found values in the coordinates $\ln \dot{e} \sim \ln \sigma_p$ (see Eq. (2)), and for a chosen low-temperature level (i.e. for high stress values) the constant β is obtained by the linear regression in the coordinates $\ln \dot{e} \sim \sigma_p$ (see Eq. (3)). After the calculation of the quantity α, the constants Q and C in the Eq. (1) can be calculated by the final linear regression of all the data plotted in the coordinate system $\ln \dot{e} - n \cdot \ln(\sinh(\alpha \cdot \sigma_p)) \sim T^{-1}$. Only the universal Eq. (1) can describe the σ_p values for any value of the product $(\alpha \cdot \sigma_p)$.

At the beginning of the activation energy calculations, the alpha value is not known. Therefore, σ_p values measured at the highest and lowest testing temperature levels are commonly used for the calculations of the constants in Eqs. (2) and (3). Such an estimate of constants n and β is a weak point of the

[1] VSB – TECHNICAL UNIVERSITY OF OSTRAVA, FACULTY OF MATERIALS SCIENCE AND TECHNOLOGY, 17. LISTOPADU 2172/15, 708 00 OSTRAVA-PORUBA, CZECH REPUBLIC
[2] SILESIAN UNIVERSITY OF TECHNOLOGY, FACULTY OF MATERIALS ENGINEERING AND METALLURGY, 8 KRASIŃSKIEGO STR., 40-019 KATOWICE, POLAND

* Corresponding author: ivo.schindler@vsb.cz

described method, since it can be strongly influenced by the selection of the corresponding temperature levels. This was previously demonstrated, for example, by calculating the Q values of 456-570 kJ · mol^{-1} for the Fe-40Al + TiB_2 alloy [6]. Values of n and β constants can vary considerably for a given material when calculated for different temperature levels – recently see e.g. [7-10]. This deficiency can be eliminated by the application of the specially developed software ENERGY 4.0 [6] which uses the aforementioned values of n and β only as the first estimate of parameters for the final refining nonlinear regression analysis of all the data corresponding to Eq. (1).

Calculation of the hot deformation activation energy from experimental σ_p-values on the basis of the hyperbolic-sine Eq. (1) is an established method that was successfully applied for different types of materials, recently for example for various types of steel [11-13], intermetallic compounds [14], alloys based on copper [15,16], titanium [17,18] or magnesium [19,20], etc. The use of the peak stress σ_p seems to be physically justified in this case, because for different Z-parameter values it corresponds to qualitatively similar structural states given by the initiation of dynamic recrystallization; similarly, in the case of the stress σ_{ss} (MPa) corresponding to steady state. A peak in the stress-strain curve means the dynamic balance between deformation strengthening and dynamic softening processes. The critical strain for the onset of dynamic recrystallization is closely related to the peak coordinate. The steady state strain can be considered as deformation at which the dynamic recrystallization becomes complete [21-23]. It is questionable whether the Q-value is indeed constant over a continuous hot deformation when there are considerably different proportions of deformed and recrystallized grains at different strain values. By modifying Eq. (1), general dependence of the stress σ (MPa) on parameter $Z = \dot{e} \cdot \exp(Q/(R \cdot T))$ can be expressed [1,2]:

$$\sigma = \frac{1}{\alpha} \cdot \ln\left[\left(\frac{Z}{C}\right)^{\frac{1}{n}} + \sqrt{\left(\frac{Z}{C}\right)^{\frac{2}{n}} + 1}\right] = \frac{1}{\alpha} \cdot \operatorname{arcsinh}\sqrt[n]{\frac{Z}{C}} \qquad (4)$$

Equation (4) represents the relationship which is often used to approximate hot flow curves in the wide range of thermomechanical conditions. In order to use Eq. 4 for the description of flow stress in the whole range of deformation, it is necessary to express the quantities A, n, Q and α as parameters dependent on true strain e (-). These dependencies are considered by several authors to be polynomials (most often of the 4th or 5th order), thus having a phenomenological character – see e. g. [24-26]. This indicates a significant effect of the strain value on the Q parameter, which would generally not be considered a material constant. Liu et al. [27] even describe the dependence of activation energy on strain, strain rate and temperature, and moreover, the situation can be complicated by calculating the true activation energy value (defined differently from apparent hot activation energy) [28].

The aim of the work was to determine the effect of strain on apparent hot deformation activation energy and to confirm it or refute it on the basis of the mathematical analysis of the available experimental data sets. In doing so, the values of the activation energy calculated from the stress σ_p and σ_{ss} were compared. The quantities further marked as Q_p (J · mol^{-1}) and Q_{ss} (J · mol^{-1}) are corresponding to significantly different values of true strain. Furthermore, in the case of selected alloy, the Q values corresponding to different e-values regarding to the wide strain range of flow curves have also been studied.

2. Processing of experimental data

In the database of own results (for a total of 6 alloys) and in literary sources (for the next 5 alloys), stress-strain curves were found, for specific materials suitable for reliable localization of the σ_p and σ_{ss} values. This required working with materials exhibiting a sufficiently rapid onset of dynamic recrystallization under the experimental conditions and transitioning into a steady state with constant stress level. The data obtained by uniaxial compression tests for quite small strain rates and/or high temperatures mostly suited it. The stress-strain curves obtained at higher values of the Zener-Hollomon parameter were often unusable for this purpose because they showed no distinct steady state stress. This, of course, is in some contradiction with operating conditions, where the hot forming is mostly realized at relatively high strain rates. The σ_p and σ_{ss} values were obtained from other authors by digitizing the published stress-strain curves. Only sufficiently comprehensive sets of experimental data were used, corresponding to a larger temperature-compensated strain rate range. The Q_p and Q_{ss} values were calculated for each material by methodology described above (using ENERGY 4.0 software) based on the same number of curves with evident σ_p and σ_{ss} stress coordinates – to ensure comparability of results for individual alloys. Since there are some stress changes even in the steady state, the σ_{ss} values were determined by linear regression of the relevant data (parallel to the horizontal axis). Data on curves not showing unambiguous steady-state data had to be excluded from data files. Therefore, the Q_p values did not always follow the values previously obtained by mathematical processing of the complete set of curves. There are basic characteristics and chemical compositions on alloys in Table 1, for which Q_p, Q_{ss} values and other constant in Eq. (4) have been calculated. The own results (marked as O) were obtained on the hot deformation simulator Gleeble 3800 in VSB-TU Ostrava.

Table 2 gives a precise description of the deformation conditions of the individual alloys and the respective stress-strain curves (always defined by the temperature and strain rate values). Table 3 includes the activation energy values and all other constants in Eq. (4) calculated in two variants – for peak (p) and steady state (ss).

3. Discussion of results

The discrepancy between Q_p and Q_{ss} values should be due to different dislocation density and grain character. Charts on

TABLE 1

Description of the processed alloys

Material	Characterization	Chemistry in wt.%	Ref.
Alloy 1	low carbon steel	Fe-0.036C-0.29Mn-0.04Si	O
Alloy 2	medium carbon steel microalloyed with V and Ti	Fe-0.34C-1.52Mn-0.72Si-0.083V-0.018Ti-0.0114N	[29]
Alloy 3	medium carbon steel microalloyed with Ti and B	Fe-0.30C-1.20 Mn-0.22Si-0.022Ti-0.0032B	O [11]
Alloy 4	medium carbon steel C45	Fe-0.49C-0.76Mn-0.28Si	O
Alloy 5	modified H13 hot work tool steel	Fe-0.49C-5.15Cr-1.26Mo-0.84V	[30]
Alloy 6	low-density austenitic steel	Fe-0.8C-17Mn-8Al	[31]
Alloy 7	copper alloy CuCr0.6	Cu-0.6Cr-0.1P	O
Alloy 8	magnesium alloy AZ31	Mg-2.82Al-0.80Zn-0.37Mn	[19,32]
Alloy 9	duplex near alpha titanium alloy Ti6242	Ti-5.7Al-2.0Mo-4.1Zr-2.0Sn-0.08Si	[33]
Alloy 10	nickel alloy Inconel 600	Ni-16.0Cr-9.2Fe-0.21Ti-0.073C	O
Alloy 11	nickel alloy Incoloy 825	Ni-30.0Fe-22.5Cr-3.4Mo-1.7Cu-1.2Ti-0.2Al-0.013C	O

TABLE 2

Deformation parameters of the analyzed flow stress curves

Material	Deformation temperature and strain rate values
Alloy 1	1523 K (0.05 – 1 – 20 s^{-1}), 1423 K (0.05 – 1 – 20 s^{-1}),
	1323 K (0.05 – 1 s^{-1}), 1323 K (0.05 – 1 s^{-1})
Alloy 2	1423 K (0.003 – 0.01 – 0.03 – 0.1 s^{-1}), 1373 K (0.003 – 0.01 – 0.03 – 0.1 – 0.3 s^{-1}),
	1323 K (0.003 – 0.01 – 0.05 – 0.1 – 0.3 s^{-1}), 1273 K (0.005 – 0.01 – 0.05 – 0.3 s^{-1})
Alloy 3	1473 K (0.1 – 1 – 11 s^{-1}), 1373 K (0.1 – 1 – 11 s^{-1}),
	1273 K (0.1 – 1 – 10 s^{-1}), 1173 K (0.1 – 1 – 10 s^{-1})
Alloy 4	1553 K (0.05 – 1 – 20 s^{-1}), 1393 K (0.05 – 1 – 20 s^{-1}),
	1273 K (0.05 – 1 – 20 s^{-1}), 1173 K (0.05 – 1 – 20 s^{-1})
Alloy 5	1423 K (0.01 – 0.1 – 1 s^{-1}), 1373 K (0.01 – 0.1 s^{-1}), 1323 K (0.01 – 0.1 – 1 s^{-1}),
	1273 K (0.01 s^{-1}), 1223 K (0.1 – 1 s^{-1}), 1173 K (1 s^{-1})
Alloy 6	1373 K (0.001 – 0.01 – 0.1 – 1 s^{-1}), 1273 K (0.001 – 0.1 – 1 s^{-1}),
	1173 K (0.001 – 0.1 s^{-1}), 1073 K (0.01 s^{-1}), 973 K (0.001 – 0.01 s^{-1})
Alloy 7	1223 K (0.1 – 1 – 10 s^{-1}), 1123 K (0.1 – 1 – 10 s^{-1}),
	1023 K (0.1 – 1 – 10 s^{-1}), 923 K (0.1 – 1 s^{-1})
Alloy 8	723 K (0.01 – 0.1 – 1 s^{-1}), 673 K (0.01 – 0.1 – 1 s^{-1}),
	623 K (0.01 – 0.1 s^{-1}), 573 K (0.01 – 0.1 s^{-1})
Alloy 9	1273 K (0.003 – 0.03 – 0.3 s^{-1}), 1173 K (0.03 – 0.3 s^{-1}),
	1073 K (0.03 – 0.3 s^{-1}), 973 K (0.03 – 0.3 s^{-1})
Alloy 10	1513 K (0.1 – 2 – 30 s^{-1}), 1373 K (0.1 – 2 – 30 s^{-1}),
	1253 K (2 – 30 s^{-1}), 1153 K (0.1 – 2 – 30 s^{-1})
Alloy 11	1513 K (0.1 – 2 – 30 s^{-1}), 1373 K (0.1 – 2 – 30 s^{-1}), 1253 K (0.1 – 2 – 30 s^{-1}),
	1153 K (0.1 – 2 – 30 s^{-1}), 1073 K (0.1 – 2 – 30 s^{-1})

TABLE 3

Material constants calculated for individual alloys

Material	Q_p	Q_{ss}	n_p	n_{ss}	α_p	α_{ss}	C_p	C_{ss}
	(kJ·mol^{-1})	(kJ·mol^{-1})	(-)	(-)	(MPa^{-1})	(MPa^{-1})	(s^{-1})	(s^{-1})
Alloy 1	318	297	5.01	4.18	0.0104	0.0115	1.6E+12	3.1E+11
Alloy 2	369	384	6.13	5.67	0.0074	0.0107	6.2E+14	4.4E+14
Alloy 3	315	281	5.90	5.31	0.0054	0.0004	6.7E+13	6.8E+18
Alloy 4	296	279	4.71	4.40	0.0079	0.0083	9.7E+11	3.0E+11
Alloy 5	437	396	5.97	4.33	0.0060	0.0084	4.7E+16	2.5E+14
Alloy 6	434	404	5.05	5.08	0.0060	0.0062	1.6E+17	1.2E+16
Alloy 7	340	393	5.60	5.78	0.0218	0.0261	6.0E+14	6.4E+16
Alloy 8	163	141	7.20	4.61	0.0068	0.0302	1.6E+15	1.2E+09
Alloy 9	575	613	2.05	4.08	0.0142	0.0075	5.9E+22	7.6E+25
Alloy 10	494	474	4.62	3.77	0.0076	0.0097	6.1E+17	7.3E+16
Alloy 11	601	501	4.15	4.04	0.0095	0.0085	1.1E+21	1.1E+18

Figs. 1 and 2 document that Q_{ss} values are on average about 6% lower than Q_p values and that a linear dependence was found between them. On the basis of the partial correlation calculations, a still weak dependence between n_p a n_s values was revealed (see Fig. 3), but no other dependencies of quantities in Table 3 were reflected.

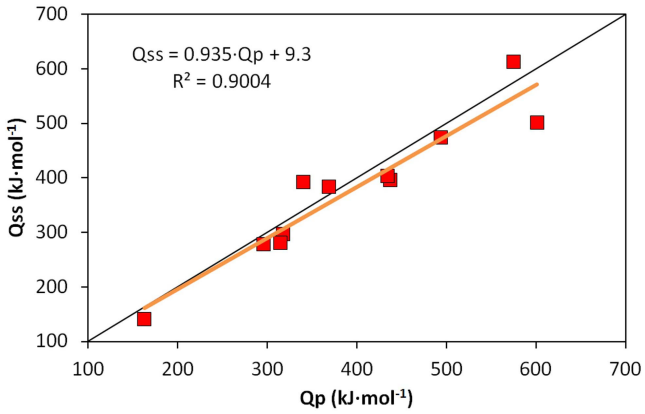

Fig. 1. Linear dependence of the Q_{ss} and Q_p values

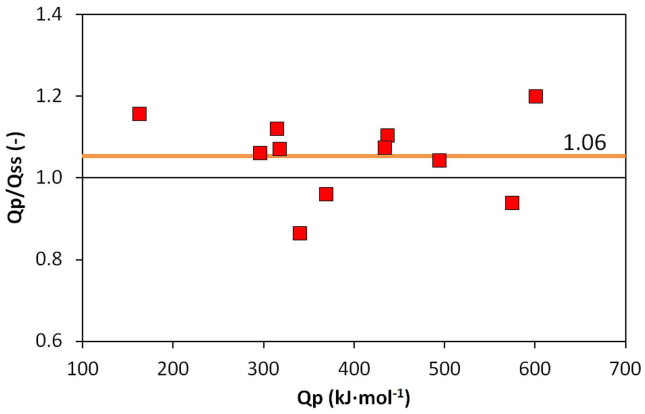

Fig. 2. Representation of the average deviation of Q_{ss} and Q_p values

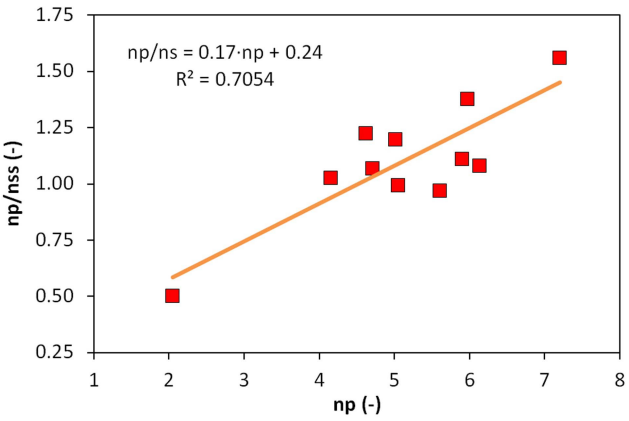

Fig. 3. Description of the relationship between n_p and n_s values

Several authors have calculated apparent hot deformation activation energy for different materials for graded strains, not only on the basis of σ_p and σ_{ss} quantities. Their digitized results are shown graphically in Fig. 4 for Ti-6Al-4V titanium alloy [2], T24 ferritic steel [26], 17-4 PH stainless steel [34], and Q420qE microalloyed steel [35].

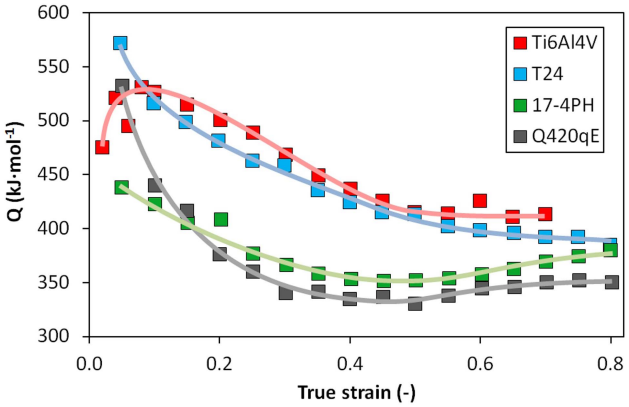

Fig. 4. Effect of deformation on the Q value of selected steels and titanium alloy

In most cases, the activation energy decreases more or less with increasing plastic deformation, which is consistent with the data in Table 3. However, the relative differences of Q values within individual materials are higher – ranging from 24% to 61%. Qualitatively similar results were achieved for 42CrMo steel [24] and for a Ti-modified austenitic stainless steel [25] as well. On the other hand, different dependence patterns were recorded for AZ81 magnesium alloy [36] and selected Al-based materials [10,27] – see Fig. 5. It is likely that this different deformation behavior is associated with other mechanisms and processes taking place in the formed material (twinning and dynamic recovery unlike recrystallization).

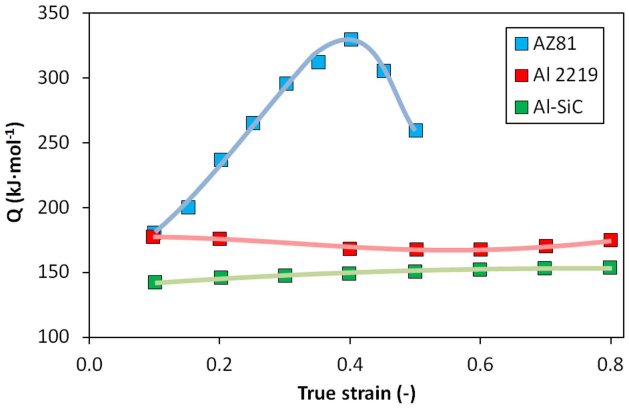

Fig. 5. Effect of deformation on the Q value of selected aluminium and magnesium based materials

In the Opěla's PhD thesis [37], Q values and other parameters in Eq. (4) were calculated for C45 steel (i.e. Alloy 4 in Table 1) by the methodology described above, but based on a different set of experimental data. Total of 20 flow curves were obtained for combination of temperature 1173 K – 1273 K – 1373 K – 1473 K – 1553 K and nominal strain rate 0.1-1.0 – 10 – 100 s^{-1} (see Fig. 6 for example).

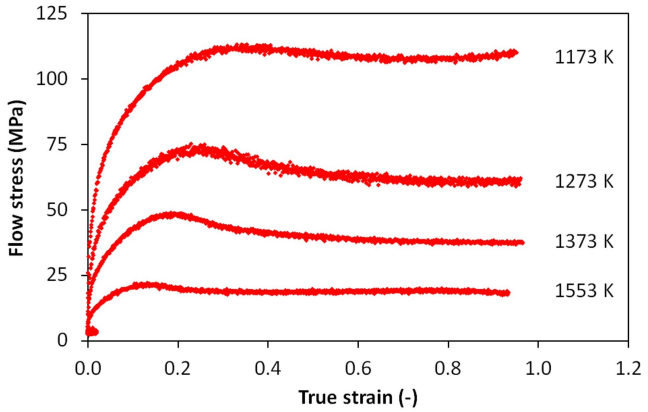

Fig. 6. Selected stress-strain curves of C45 steel (strain rate 0.1 s^{-1}) – according to [38]

Figure 7 clears that, with the exception of small strains, the Q and n values decrease with increasing deformation, but after exceeding true strain of $e = 0.4$, they are more or less stabilized. It is worth noting a much greater dispersion of the calculated values in the case of activation energy. Difference in Q values in Fig. 7 and in Table 3 for Alloy 4 is defined by the difference of the default data sets (with much lower strain rates in the case of Table 3). After smoothing the dependencies in Fig. 7, the difference between the highest and lowest Q is about 8%, which is in accordance with the average difference of 6% between Q_p and Q_{ss} values in Table 3.

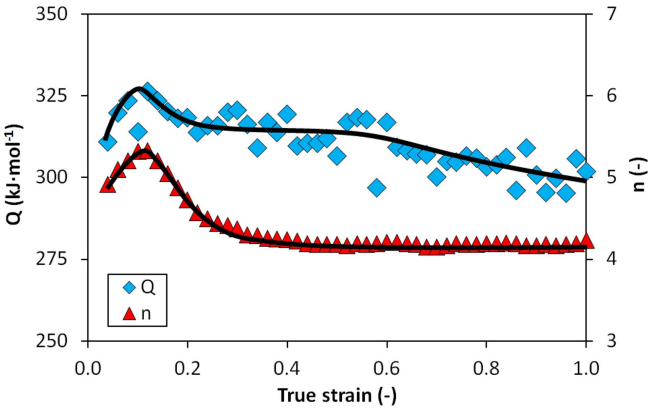

Fig. 7. Influence of deformation on Q and n quantities for C45 steel

Activation energy Q_p values can be applied, for example, in physically based phenomenological models of the hot flow stress [11,38,39]. These are then used for more precise prediction of the forming forces in rolling mills and forges.

It should be noted that all of the activation energy calculations described herein were based on the apparent constitutive analysis. Mirzadeh, Saadatkia and other researchers [40-42] have described the possibilities and advantages of physically based constitutive analysis which accounts for the temperature dependence of the Young's modulus and the self-diffusion coefficient of austenite. Such an approach directly deals with the atomic mechanisms.

4. Conclusions

- Flow stress curves significantly affected by dynamic recrystallization were analyzed for 11 different iron, copper, magnesium, titanium or nickel based alloys. Based on stress values of clearly unequivocal peak stress or steady-state stress (i.e. σ_p and σ_{ss}), apparent hot deformation activation energy Q_p and Q_{ss} values were calculated.
- A linear dependence between Q_p and Q_{ss} was found, where Q_p values are on average only about 6% higher. This was also confirmed by calculating the dependence of activation energy on true strain (up to $e = 1$) in C45 medium carbon steel, where the largest difference in Q values was about 8%.
- Correlation analysis revealed no further significant dependencies between other parameters in the sinus-hyperbolic relationship, used mainly for prediction of peak stress depending on Zener-Hollomon parameter Z.
- The achieved results confirm that the hot deformation activation energy is to some extent influenced by the strain value and strictly speaking it is not a material constant, but its minor changes may not play a key role in the prediction of flow stress $\sigma = f(e, Z)$.

Acknowledgements

The paper was created thanks to the project No. CZ.02.1.01/0.0/0.0/17_049/0008399 (from the EU and CR financial funds provided by the Operational Programme Research, Development and Education, Call 02_17_049 Long-Term Intersectoral Cooperation for ITI), and the students grant projects SP2019/86 and SP2019/43 at VSB-TUO; managing authority: Czech Republic – Ministry of Education, Youth and Sports.

REFERENCES

[1] C. Zener, J.H. Hollomon, J. Appl. Phys. **15** (1), 22-32 (1944), DOI: 10.1063/1.1707363.

[2] M.A. Shafaat, H. Omidvar, B. Fallah, Mater. Des. **32** (10), 4689-4695 (2011), DOI: 10.1016/j.matdes.2011.06.048.

[3] I. Schindler, R. Kawulok, H. Kulveitová, P. Kratochvíl, V. Šíma, M. Knapiński, Acta Phys. Pol. A. **122** (3), 610-613 (2012), DOI: 10.12693/APhysPolA.122.610.

[4] C.M. Sellars, W.J. McG. Tegart, International Metallurgical Reviews. **17** (1), 1-24 (1972), DOI: 10.1179/IMTLR.1972.17.1.1.

[5] H.J. McQueen, S. Yue, N.D. Ryan, E. Fry, J. Mater. Process. Technol. **53** (1-2), 293-310 (1995), DOI : 10.1016/0924-0136(95)01987-P.

[6] I. Schindler, P. Kawulok, R. Kawulok, E. Hadasik, D. Kuc, High Temp. Mater. Processes. **32** (2), 149-155 (2013), DOI: 10.1515/htmp-2012-0106.

[7] T. Li, G. Liu, M. Xu, B. Wang, T. Fu, Z. Wang, R.D.K. Misra, Materials **11**, 2044 (2018), DOI: 10.3390/ma11102044.

[8] R. Gujrati, C. Gupta, J.S. Jha, S. Mishra, A. Alankar, Mater. Sci. Eng. A **744**, 638-651 (2019), DOI: 10.1016/j.msea.2018.12.008.

[9] X. Qian, N. Parson, X.G. Chen, Mater. Sci. Eng. A **764**, 138253 (2019), DOI: 10.1016/j.msea.2019.138253.

[10] K.Ch. Nayak, P.P. Date, J. Mater. Eng. Perform. **28** (9), 5323-5343 (2019), DOI: 10.1007/s11665-019-04277-8.

[11] P. Kawulok, I. Schindler, R. Kawulok, P. Opěla, R. Sedláček, Arch. Metall. Mater. **63** (4), 1785-1792 (2018), DOI: 10.24425/amm.2018.125105.

[12] S. Zheng, X. Yuan, X. Gong, T. Le, A.V. Ravindra, Metall. Mater. Trans. A. **50** (5), 2342-2355 (2019), DOI: 10.1007/s11661-019-05162-8.

[13] H. Gwon, S. Shin, J. Jeon, T. Song, S. Kim, B.C. De Cooman, Metals and Materials International. **25** (3), 594-605 (2019), DOI: 10.1007/s12540-018-00224-9.

[14] V. Singh, Ch. Mondal, A. Kumar, P.P. Bhattacharjee, P. Ghosal, J. Alloys Compd. **788**, 573-585 (2019), DOI: 10.1016/j.jallcom.2019.02.207.

[15] B. Wang, Y. Zhang, B. Tian, V. Yakubov, J. An, A.A. Volinsky, Y. Liu, K. Song, L. Li, M. Fu, J. Alloys Compd. **781**, 118-130 (2019), DOI: 10.1016/j.jallcom.2018.12.022.

[16] I. Schindler, M. Sauer, P. Kawulok, K. Rodak, E. Hadasik, M.B. Jablonska, S. Rusz, V. Sevcak, Arch. Metall. Mater. **64** (2), 701-706 (2019).

[17] W. Chen, W. Zeng, J. Xu, D. Zhou, S. Wang, S. He, J. Alloys Compd. **792**, 389-398 (2019), DOI: 10.1016/j.jallcom.2019.03.345.

[18] Q. Zhao, F. Yang, R. Torrens, L. Bolzoni, Mater. Des. **169**, 107682 (2019), DOI: 10.1016/j.matdes.2019.107682.

[19] I. Schindler, P. Kawulok, E. Hadasik, D. Kuc, J. Mater. Eng. Perform. **22** (3), 890-897 (2013), DOI: 10.1007/s11665-012-0327-8.

[20] E. Hadasik, I. Schindler, D. Kuc, T. Mikuszewski, Arch. Metall. Mater. **62** (3), 1427-1432 (2017), DOI: 10.1515/amm-2017-0220.

[21] N.D. Ryan, H.J. McQueen, J. Mater. Process. Technol. **21** (2), 177-199 (1990), DOI: 10.1016/0924-0136(90)90005-F.

[22] E.I. Poliak, J.J. Jonas, Acta Mater. **44** (1), 127-136 (1996), DOI: 10.1016/1359-6454(95)00146-7.

[23] M. Shaban, B. Eghbali, J. Mater. Sci. Technol. **27** (4), 359-363 (2011), DOI: 10.1016/S1005-0302(11)60074-1.

[24] Y.C. Lin, M.S. Chen, J. Zhong, Computational Materials Science. **42** (3), 470-477 (2008), DOI: 10.1016/j.commatsci.2007.08.011.

[25] S. Mandal, V. Rakesh, P.V. Sivaprasad, S. Venugopal, K.V. Kasiviswanathan, Mater. Sci. Eng. A. **500** (1/2), 114-121 (2009), DOI: 10.1016/j.msea.2008.09.019.

[26] H.Y. Li, D.D. Wei, J.D. Hu, Y.H. Li, S.L. Chen, Computational Materials Science. **53** (1), 425-430 (2012), DOI: 10.1016/j.commatsci.2011.08.031.

[27] L. Liu, Y.X. Wu, H. Gong, K. Wang, Trans. Nonferrous Met. Soc. China. **29** (3), 448-459 (2019), DOI: 10.1016/S1003-6326(19)64954-X.

[28] S. Wang, J.R. Luo, L.G. Hou, J.S. Zhang, L.Z. Zhuang, Mater. Des. **113**, 27-36 (2017), DOI: 10.1016/j.matdes.2016.10.018.

[29] H. Mirzadeh, J.M. Cabrera, J.M. Prado, A. Najafizadeh, Mater. Sci. Eng., A. **528** (10/11), 3876-3882 (2011), DOI: 10.1016/j.msea.2011.01.098.

[30] Ch. Li, Y. Liu, Y. Tan, F. Zhao, Metals. **8** (10), 846 (2018), DOI: 10.3390/met8100846

[31] A. Mohamadizadeh, A. Zarei-Hanzaki, H.R. Abedi, Mech. Mater. **95**, 60-70 (2016), DOI: 10.1016/j.mechmat.2016.01.001

[32] D. Kuc, E. Hadasik, I. Schindler, P. Kawulok, R. Śliwa, Arch. Metall. Mater. **58** (1), 151-156 (2013), DOI: 10.2478/v10172-012-0166-5.

[33] M. Rezaee, A. Zarei-Hanzaki, M. Ghambari, P.D. Nezhadfar, E. Ghasemi, Adv. Eng. Mater. **18** (6), 1075-1085 (2016), DOI: 10.1002/adem.201500426.

[34] H. Mirzadeh, A. Najafizadeh, Mater. Sci. Eng. A. **527** (4/5), 1160-1164 (2010), DOI: 10.1016/j.msea.2009.09.060.

[35] B.J. Yu, X.J. Guan, L.J. Wang, J. Zhao, Q.Q. Liu, Y. Cao, J. Cent. South Univ. Technol. **18** (1), 36-41 (2011), DOI: 10.1007/s11771-011-0655-0.

[36] P. Changizian, A. Zarei-Hanzaki, A.A. Roostaei, Mater. Des. **39**, 384-389 (2012), DOI: 10.1016/j.matdes.2012.02.049.

[37] P. Opěla, PhD thesis, Popis deformačního odporu za tepla v širokém intervalu termomechanických podmínek [Hot Flow Stress Description in the wide range of thermomechanical conditions], VSB – Technical University of Ostrava, Czech Republic (2017).

[38] P. Opěla, I. Schindler, P. Kawulok, F. Vančura, R. Kawulok, S. Rusz, T. Petrek, Metalurgija **54** (3), 469-472 (2015).

[39] P. Opěla, I. Schindler, P. Kawulok, F. Vančura, R. Kawulok, S. Rusz, in: Metal 2016, Ostrava: Tanger Ltd, 458-463 (2016).

[40] H. Mirzadeh, J. M. Cabrera, A. Najafizadeh, Acta Mater. **59** (16), 6441-6448 (2011), DOI: 10.1016/j.actamat.2011.07.008.

[41] H. Mirzadeh, Mater. Chem. Phys. **152**, 123-126 (2015), DOI: 10.1016/j.matchemphys.2014.12.023.

[42] S. Saadatkia, H. Mirzadeh, J.M. Cabrera, Mater. Sci. Eng. A **636**, 196-202 (2015), DOI: 10.1016/j.msea.2015.03.104.